# THE RESERVE TO THE PARTY OF THE

### Tanzania Journal of Science

Volume 51(3), 2025





Comparative evaluation of dicyclohexylamine and *N*-methyldiethanolamine as corrosion inhibitors for top of line corrosion on API X80 carbon steel in saturated carbon dioxide aqueous solutions

Frida W Andalu<sup>1\*</sup>, Abraham K Temu<sup>2</sup>, Alfred R Akisanya<sup>3</sup> and Joseph YN Philip<sup>4</sup>

### **Keywords**

Volatile corrosion inhibitor; Potentiodynamic polarization; API X80 carbon steel; Corrosion rate; Top of line corrosion.

### Abstract

This work has evaluated the efficiency of selected volatile corrosion inhibitors in mitigation of top of line corrosion in wet gas pipeline at different temperatures. The main challenge of top of line corrosion in carbon dioxide rich environment is the ability of the volatile corrosion inhibitor to effectively mitigate corrosion at adverse conditions. Electrochemical corrosion experiments using potentiodynamic polarization method were conducted at temperatures of 20 °C, 35 °C and 45 °C to evaluate the efficiency of dicyclohexylamine and n-methyldiethanolamine corrosion inhibitors for top of line corrosion inhibition on carbon steel specimens derived from API X80 natural gas pipelines. The electrolyte used, was an aqueous solution saturated with carbon dioxide, containing 200 ppm acetic acid and 1% NaCl solution, mimicking the corrosive environment in wet natural gas transportation. The results obtained show that the trend of corrosion inhibition efficiency decreased with increasing temperature such that the efficiency of 39.61%, 34.03% and 13.98% was achieved with dicyclohexylamine application and the efficiency of 34.53%, 15.30% and 6.26% was achieved with n-methyldiethanolamine at 20 °C, 35 °C and 45 °C respectively. It was observed that dicyclohexylamine behaved as an anodic inhibitor while *n*-methyldiethanolamine exhibited cathodic inhibition behaviour. In conclusion, dicyclohexylamine was an effective volatile corrosion inhibitor over *n*-methyldiethanolamine for the selected steel in CO<sub>2</sub>-saturated environments at low temperatures below 35 °C.

### Introduction

Corrosion is the process of metal deterioration caused by а chemical or electrochemical reaction with the Corrosion in gas environment. pipelines is a result of the presence of some non-hydrocarbons such as water, carbon

dioxide and hydrogen compounds that occur in line with the hydrocarbons during natural gas production (Amani and Hjeij 2015, Ituen and Asuquo 2019). When natural gas flows through the pipelines, these non-hydrocarbons condense at top inner part of pipelines and develop corrosive

Received 5 May 2025, Revised 17 August 2025, October 19 2025, Published October 30 2025 https://doi.org/10.65085/2507-7961.1059

© College of Natural and Applied Sciences, University of Dar es Salaam, 2025 ISSN 0856-1761, e-ISSN 2507-7961

<sup>&</sup>lt;sup>1</sup>Department of Petroleum Science and Engineering, University of Dar es Salaam, Tanzania

<sup>&</sup>lt;sup>2</sup>Department of Chemical and Process Engineering, University of Dar es Salaam, Tanzania

<sup>&</sup>lt;sup>3</sup>School of Engineering, University of Aberdeen, The United Kingdom

<sup>&</sup>lt;sup>4</sup>Department of Chemistry, University of Dar es Salaam, Tanzania

<sup>\*</sup> Corresponding author: <u>frida.andalu@udsm.ac.tz</u>

environments. The commonly used pipelines in the transportation of oil and gas include the steel grades such as API 5L X70, X80, X60, X65, X52, and X42 (Ituen and Asuquo 2019), these are made of carbon steel due to metallurgical and economic reasons.

Surface coating remains one of the most widely employed and effective strategies for mitigating corrosion in natural gas pipelines (Kolawole et al. 2018, Nan 2021). However, as protective coating degrades over time, recoating becomes necessary part of routine preventive maintenance. pipelines applying internal coatings to in-service pipelines possess a significant challenge due to limited accessibility and operational constraints (Niu and Cheng 2008). Consequently, the internal surfaces around pipeline joints are often left uncoated, making them particularly vulnerable to corrosion, which can accelerate structural degradation and lead to premature pipeline failure (Bai and Qiang 2014, Wint and Williamson 2014, Wang 2022).

Internal corrosion in pipelines transporting hydrocarbons is influenced by multiple factors, including temperature, the presence of CO<sub>2</sub>, H<sub>2</sub>S and water content, flow velocity, hydrocarbon composition, and the surface condition of the pipeline materials (Abbas et al. 2023, Popoola et al. 2013) top of line corrosion is a result of condensation of acidic vapours on the internal upper walls of a horizontal or near horizontal pipeline due to heat exchange between the pipeline and the surroundings (Al-Moubaraki and Obot 2021). When temperature is high, the acidic vapour is formed and goes to the upper surface of the pipeline which then condenses as cooling occurs due to temperature differences between the inner and outer parts of the pipeline (Valente Jr et al. 2020). In wet gas pipelines, high-temperature regions located at the pipeline inlet, with temperature gradually decreasing along the pipeline length depending on the effectiveness of the pipeline thermal insulation. According to Wang (2022), the decrease in temperature along the pipeline is proportional to a decrease in the rate of condensation and hence top-of-line corrosion (Wang 2022). The TLC is a major concern in the oil and gas industry due to its typically higher corrosion rates at the upper sections of the pipelines compared to the lower sections. This phenomenon is primarily attributed to the accumulation of corrosive species such as water vapour and acid gases at the top of the pipe, where condensation is more likely to occur. Among other corrosion inhibition techniques, volatile corrosion inhibitors have been used to mitigate top of line corrosion in gas pipelines because they can be vaporized and form a protective layer on metal surfaces, preventing corrosive agents from reaching the metal (Ramlan et al. 2024).

Corrosion inhibitors impede corrosion process by forming a protective layer on the metal surface through absorption of the the corrosion molecules of inhibitor. Coordinate bonds are formed when these molecules donate electrons to the vacant dorbital of the metal (Mungwari et al. 2024). During corrosion process, metal atoms are oxidized, and their ions are transferred from the anode in the solution to the cathode. The cathodic process requires hydrogen ion as an electron acceptor and oxygen as an oxidizing agent. Corrosion can be minimized by impeding the anodic or cathodic reactions using inhibitors whose molecules can be absorbed on the surface. The inhibitors interact with cathodic, anodic, or both sites and decrease the reduction, oxidation, or both corrosive reactions that are taking place on the metal surface (Abbas et al. 2023).

The recent published article by Zankana et al. (2023) conducted a comparative study of corrosion inhibitors named novel nitrogen doped carbon dots, imidazole-citric acidbased carbon dots and novel N-doped carbon dots on O235 carbon steel using different techniques (Zankana et al. 2023). The techniques involved were Scanning probe transmission microscope, electron microscopy and X-rav photoelectron spectroscopy to investigate the chemical composition of the adsorbed surface.

Eslami and Singer (2023) investigated the injection of the volatile corrosion inhibitor into pipelines. The volatile corrosion inhibitor was introduced into a system comprising two

interconnected glass cells to simulate the pipeline environment. The findings indicated that the phase of volatile corrosion inhibitor injection, whether gas or liquid, does not affect the inhibition efficiency.

Research on amine-based volatile corrosion inhibitors, particularly for mitigating top-ofline corrosion in carbon steel pipelines within the oil and gas industry, remains limited (Belarbi et al. 2016, Gunasekarana et al. 2016, Ramlan et al. 2024, Al-Moubaraki and Obot 2025). N-methyldiethanolamine commonly employed corrosion inhibitor with other film forming corrosion inhibitor as part of a corrosion control program to go alongside to inhibit hydrate formation in gas pipelines (Alef and Barifcani 2020). Also, dicyclohexylamine which is also a common volatile corrosion inhibitor has been studied in its salt form of dicyclohexylamine nitrite (Khamis et al. 2001, Cano et al. 2005) and in a mixture with another amine as reported by Jevremovic et al. (2012)

In this work, electrochemical corrosion experiments to determine the efficiency of two amine-based volatile corrosion inhibitors, which are dicyclohexylamine and *n*-methyldiethanolamine were carried out to API X80 carbon steel from a natural gas

pipeline. Temperature which has been studied by Konovalova (2020) as a key parameter for corrosion inhibitors evaluation in API 5L X60 carbon steel was used as a variable parameter for this work. The electrolyte (corrosion medium) was aqueous solution saturated with carbon dioxide containing 200 ppm acetic acid and 1% NaCl, which mimic the corrosive environment in wet natural gas transportation. The findings in this work were useful to suggest the best inhibitor and its suitable operating conditions.

### Materials and Methods Materials

All chemicals used in this work were purchased from Thermo Scientific, UK including dicyclohexylamine ( $\geq 99$  %), N-methyl diethanolamine ( $\geq 98$ %), analytical sodium chloride, and acetic acid glacial ( $\geq 99$ %), and ethanol ( $\geq 99$ %), Other materials include API X80 carbon steel specimens derived from a gas pipeline material and used as working electrode, with their specifications given in Table 1, silicon carbide papers, and commercial carbon dioxide gas cylinder ( $\geq 99$ %), supreme polycrystalline diamond suspension.

Table 1: Chemical composition of the API X80 carbon steel pipeline used for transportation of natural gas (mass fraction: %)

			0		,							
Element	С	Si	Mn	P	S	Cr	Ni	V	Nb	Ti	Mo	Fe
Wt (%)	0.04	0.21	1 75	< 0.012	< 0.003	0.02	0.16	0.04	0.06	0.01	0.11	97 59

$$1$$
 HO  $N$  OH  $2$ 

**Figure 1**: The structures of dicyclohexylamine (1) and *n*-methyldiethanolamine (2) volatile corrosion inhibitors

### Preparation and analysis of the working electrode

The working electrode was obtained from carbon steel API X80 material which is commonly used for large-diameter pipelines between 24 and 36 inches for transportation of wet natural gas. Circular specimens were

prepared in the laboratory with an average diameter of 11.2 mm and thickness of 3.53 mm and modified to fit in the sample holder of the corrosion cell. All specimens were properly polished to different surface properties using silicon carbide papers of various grit sizes (120, 180, 220, 320 and

500) and MasterTex polishing cloth of MetaDi-supreme polycrystalline diamond suspension of 9  $\mu$ m and 3  $\mu$ m and 0.05  $\mu$ m in an Ecomet 250 Beuhler grinder/polisher machine to mirror surface because the smooth surface deteriorates slower than the rough surface (Afsa 2011). Each specimen was polished for 4 minutes in a particular abrasive paper using an Ecomet 250 Beuhler grinding/polishing machine and rinsed with ethanol. The specimen's surface was further analysed using the Gemini SEM 300 model scanning electron microscope coupled with an energy dispersive spectroscope.

### Deposition of volatile corrosion inhibitor

The experimental setup for volatile inhibitor deposition corrosion on the specimen surface was adapted from Skinner's test with few modifications (Hong-jing et al. 2005). The experimental setup shown in Figure 2 was devised for the evaluation of volatile corrosion inhibitor on an API X80 carbon steel specimen under conditions of temperature and constant concentration of the corrosion medium. About 20 mL of volatile corrosion inhibitor was placed in a 100 mL conical flask. In the setups, one side polished rectangular metal specimen of 11.2 mm  $\times$  3.53 mm was level mounted at the top of the flask fixed in a stopper with the specimen surface to be analysed facing the bottom of the flask with the volatile corrosion inhibitor at the bottom. The conical flask with the volatile corrosion inhibitor was inserted in a beaker with water to act as a water bath. The thermostat was inserted inside the beaker with water to control the temperature of the heat transferred in the flask with volatile corrosion inhibitor. Then the volatile corrosion inhibitor deposition experiment was subjected to heating at a constant temperature of 60 °C for 12 h to allow the volatile corrosion inhibitor to vaporize and get deposited on the surface of the metal specimen at the top of the flask. Then the heating device was switched off and the specimen was carefully handled and transferred to corrosion cell sample holder and subjected to an electrochemical corrosion test in an acidic medium.

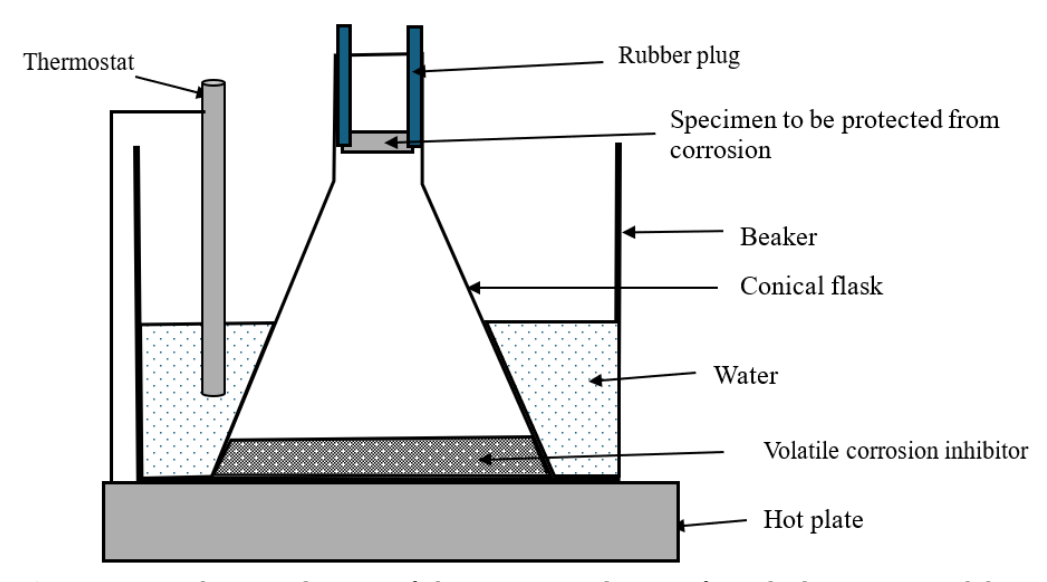


**Figure 2**: A schematic diagram of the experimental set-up for volatile corrosion inhibitor deposition on the working electrode surface under controlled temperature in a water bath

### **Electrochemical corrosion tests**

The electrochemical corrosion tests were conducted at different experimental

conditions in a three electrodes corrosion cell with a capacity of 1100 mL. Two commercial volatile corrosion inhibitors,

dicyclohexylamine and nmethyldiethanolamine were used. The electrochemical corrosion measurements were carried out using a three-electrode system connected to the EG&G Princeton Applied Research Model Potentiostat/Galvanostat. The electrodes were the X80 carbon steel specimens as the working electrode, the saturated calomel plugged to the cell externally via a Luggin capillary tube as reference electrode, and two carbon rods counter-electrode. The water bath, during corrosion tests, was cushioned by using plastic balls to reduce heat loss to environment. hence maintaining the corrosion medium temperature of constant. Before the test, CO2 gas was purged in a cell corrosion medium for about 45 minutes to ensure the corrosion medium was saturated with CO<sub>2</sub> gas while the pH ranged 2 – 3. Then the sample holder with a specimen was fixed at the middle of the corrosion cell closer to a reference electrode.

The potentiodynamic measurements were performed anodically from 
$$E = -250$$
 mV to  $E = +250$  mV against standard calomel electrode, at a scan rate of 0.1667 mV/s. Initially, the open circuit potential was allowed to stabilize for about 45 minutes. The polarisation curves analysed and the linear regions of the Tafel plots, cathodic and anodic curves were manually fitted to obtain corrosion parameters such as corrosion potential ( $E_{corr}$ ), corrosion current density ( $i_{corr}$ ), Tafel slopes ( $\beta_c$  and  $\beta_a$ ). The obtained polarization curves and electrochemical parameters for different tests were used to compare the efficiency of each volatile corrosion inhibitor with respect to the conditions of the experiment.

Corrosion rates were calculated by assuming a uniform corrosion that anodic and cathodic reactions take place all over the electrode surface using Equation (1).

$$CR = \frac{315 \, Wi_{corr}}{nF \, \rho} \tag{1}$$

where  $i_{corr}$  is corrosion current density ( $\mu$ A/cm<sup>-2</sup>), W is atomic mass of the metal ( $g \cdot mol^{-1}$ ),  $\rho$  (= 7.86  $g \cdot cm^{-3}$ ) is density of the metal, and F (= 96,485 C.mol<sup>-1</sup>) is the Faraday constant and CR is corrosion rate in mmpy (mm per year).

The corrosion inhibition efficiency (  ${\it IE}$  ) was calculated using Equation 2.

$$IE = \frac{i_{corr}^{\circ} - i_{corr}}{i_{corr}^{\circ}} \times 100$$
(2)

where  $i_{corr}$  and  $i_{corr}$  are the corrosion current density for specimens without and with volatile corrosion inhibitor and, respectively.

### Results and Discussion Analysis of the API X80 carbon steel working electrodes

The surface property of the material is essential for effectiveness of a corrosion inhibitor. Volatile corrosion inhibitors are most effective on a uniform and clean metal surface. Non-uniform surface morphology can hinder the even adsorption of volatile corrosion inhibitors, thereby compromise protective film formation and increase susceptibility to localized corrosion. The

surface of the corrosion coupon was examined before deposition of the volatile corrosion inhibitor and the corrosion test. The scanning electron microscope image of the polished specimen surface with some minor micron-sized inclusions before corrosion test shown in Figure 3(a), corresponding energy dispersive spectrum. The energy dispersive spectra are shown in Figure 3(b) and spectrum 4 in Figure 3(c). Energy dispersive Spectrum 3 undertaken away from the inclusions, while Andalu et al. - Comparative Evaluation of Dicyclohexylamine and N-Methyldiethanolamine as Corrosion Inhibitors ...

spectrum 4 was captured within an inclusion. The energy dispersive spectrum in Figure 3(b) revealed element composition (wt.%): Si (0.27); Mn (1.46); Mo (0.27), C (0.277), and Fe (97.7), while the elemental composition (wt.%) within the inclusion (Figure 3(c)) were found to be O (39.27), Mg (18.78), Al (10.04), Si (0.05), S (9.39), Ca (17.09), and Fe (5.38). Elevated levels of magnesium, aluminium, calcium and oxygen in energy dispersive spectrum signify the existence of these metals. The presence of inclusions in carbon steel results from the incorporation of micro-alloying components during

production process to enhance mechanical properties and corrosion resistance (Xue and Cheng 2011). Studies have shown that these inclusions can facilitate pitting corrosion by serving as initiation sites for corrosion (Yonova et al. 2007). It is therefore likely that the corrosion rates result in this work may be somehow altered by the presence of magnesium, aluminium and calcium oxide metal inclusions which have been found at elevated levels compared to aluminium oxide inclusions.

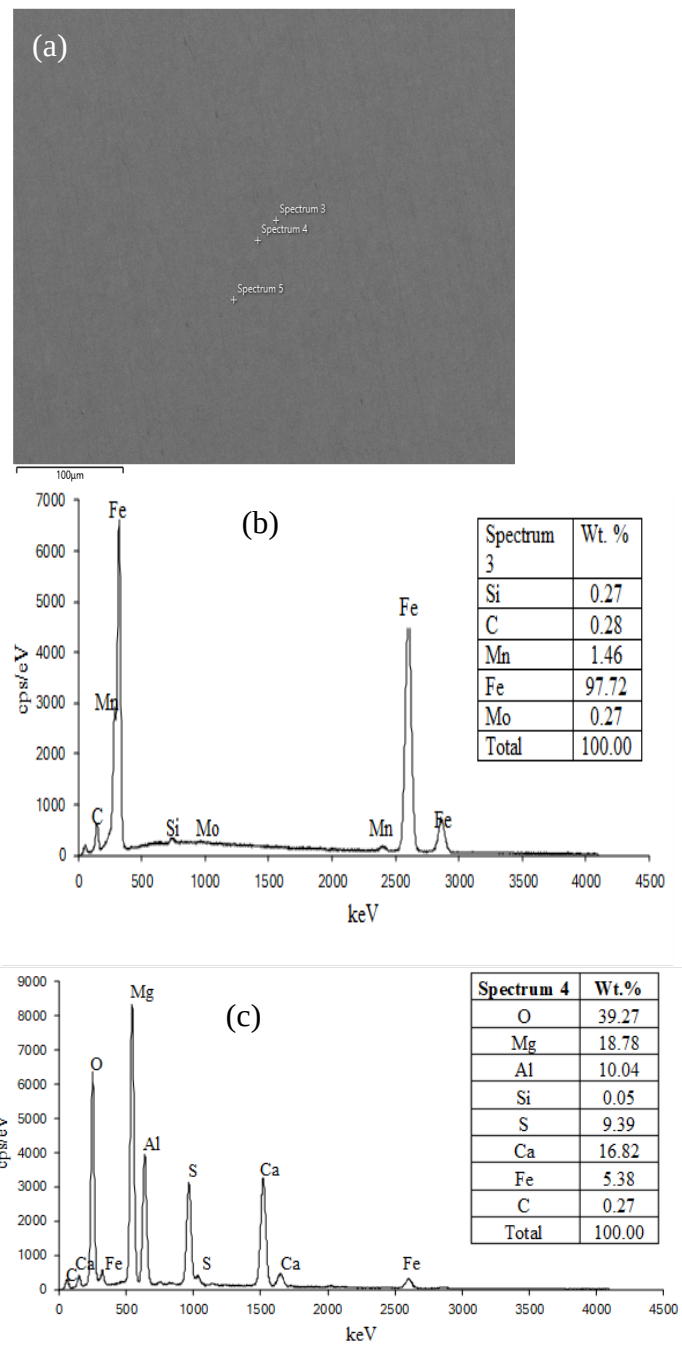


**Figure 3**: Scanning electron microscope - energy dispersive spectroscope analysis of the polished specimen surface (a) Scanning electron micrograph of a polished corrosion coupon before corrosion test, (b) Scanning electron spectrum at location labelled Spectrum 3 in scanning electron microscope image, away from inclusion, and (c) the scanning electron spectrum at location labelled Spectrum 4 in the scanning electron microscope image within an inclusion.

### The effect of temperature on the corrosion of uninhibited API X80 carbon steel

The potentiodynamic polarization curves obtained from uninhibited API X80 carbon steel specimens at different temperatures are presented in Figure 4. Generally, increase in temperature from 20  $^{\circ}$ C to 45  $^{\circ}$ C resulted in the anodic shift of the corrosion potential with more negative corrosion potential at 45  $^{\circ}$ C and decreases gradually to less negative potential at 20  $^{\circ}$ C. This indicates that

corrosion rates increase with temperature, consistent with the thermally accelerated kinetics of both anodic and cathodic reactions. The electrochemical parameters obtained from Figure 4 by extrapolation of Tafel lines are presented in Table 2. The parameters reported in this work correspond to the results reported by Shahzad et al (2020) on X120 carbon steel in saturated carbon dioxide without corrosion inhibitor on the surface.

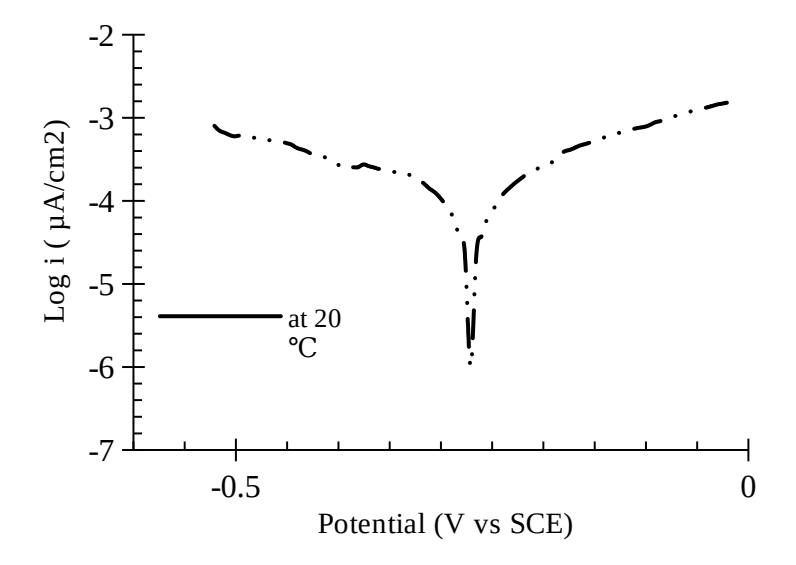


**Figure 4**: Polarization curves for API X80 carbon steel specimens recorded after 2 hours exposure in CO<sub>2</sub> saturated, 1% NaCl, 200 ppm acetic acid electrolyte on uninhibited specimen, at different temperatures

From Table 2, it is observed that  $|\beta_c|$  and  $\beta_a$  increased slightly with the increase in temperature. This is an indication that increase in temperature affect both anodic and cathodic processes. It is observed from this table that, as expected, corrosion current density increased with increase in temperature, and consequently the corrosion rate.

## The effect of temperature on inhibited and uninhibited API X80 carbon steel specimens at 20 °C

The results obtained from corrosion experiments on inhibited specimens were evaluated against uninhibited specimens to determine the efficiency of the corrosion inhibitors at 20 °C as indicated in Figure 5.

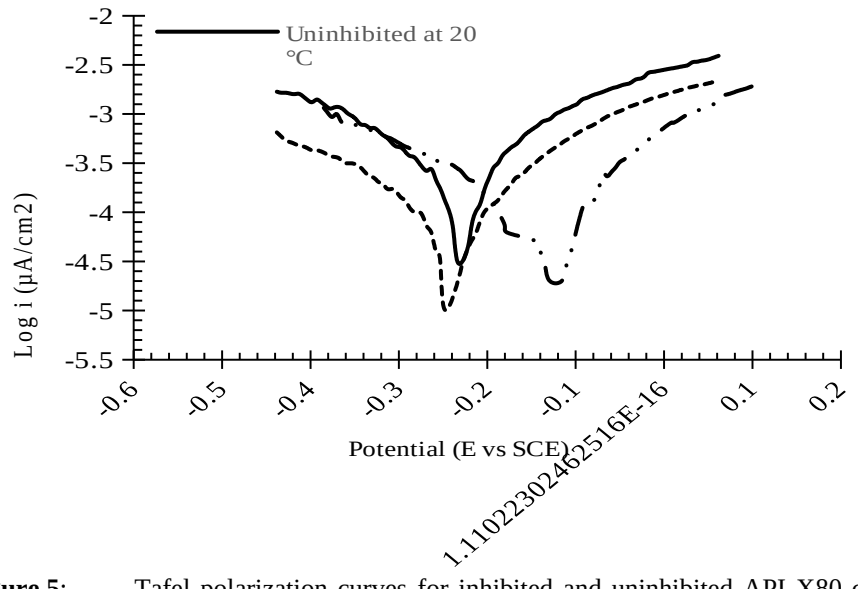


**Figure 5**: Tafel polarization curves for inhibited and uninhibited API X80 carbon steel specimens, recorded at 20 °C and specimens exposed in CO<sub>2</sub> saturated electrolyte containing 200 ppm acetic acid and 1% NaCl. MDEA = *n*-methyldiethanolamine, DCHA = dicyclohexylamine

From Figure 5, it is observed that the dicyclohexylamine and methyldiethanolamine deposition on API X80 carbon steel specimens affected both anodic and cathodic polarization curves. Corrosion tests with dicyclohexylamine inhibitor exhibited better corrosion efficiency with less negative corrosion potential as well as less corrosion rate compared to the curves with *n*-methyldiethanolamine and uninhibited specimens. This confirms successful adsorption of the inhibitor molecules on the carbon steel surfaces. At 20 °C, the presence of dicyclohexylamine on the metal surface caused the  $E_{corr}$  to shift anodically, with dicyclohexylamine being more effective, while *n*-methyldiethanolamine caused the  $E_{corr}$  to shift cathodically. The shifts of  $E_{corr}$ might be attributed by the difference in chemical structures of dicyclohexylamine and n-methyldiethanolamine as illustrated in Figure 1. Dicyclohexylamine is a water insoluble inhibitor and a surface-active agent (Jevremovic et al. 2012). This state hinders easily detachment of dicyclohexylamine from the specimen surface, hence slows down the corrosion rate. The inclusion of polar hydroxyl groups at both ends of nmethyldiethanolamine enhances its solubility in water by facilitating hydrogen bond formation with water molecules, so allowing it to be readily removed from the specimen's surface (Tong et al. 2023). The corrosion inhibition efficiencies of the volatile inhibitors in Table corrosion were calculated by using Equation (2). The efficiency of dicyclohexylamine is significant and it reflects the positive potential shift in the polarization curve. At 20 °C the corrosion rate of the carbon steel was reduced from 0.84 mmpy to 0.54 mmpy corresponding to 39.61% which is a significant reduction. With *n*-methyldiethanolamine the corrosion rate was reduced from 0.84 mmpy to 0.56 mmpy corresponding to 34.53% slightly lower than with dicyclohexylamine. In the literature however, at 20 °C and 50 ppm of dicyclohexylamine added with oleyamine in CO<sub>2</sub> saturated environment and 3% NaCl, the efficiency of 44% was reported (Jevremovic et al. 2012). These results indicate similar of performance οf the dicyclohexylamine.

Andalu et al. - Comparative Evaluation of Dicyclohexylamine and N-Methyldiethanolamine as Corrosion Inhibitors ...

Table 2: Electrochemical parameters obtained from the linear fit of Tafel plots, along with calculated corrosion rates and inhibition efficiencies for inhibited and uninhibited carbon steel API X80 specimens, exposed to a CO<sub>2</sub>-saturated 1% NaCl solution, 200 ppm acetic acid electrolyte at 20 °C, 35°C and 45 °C.

	$eta_{ m c}$	$eta_{ ext{a}}$	$E_{ m corr}$	$i_{ m corr}$	CR	IE (%)					
	(mV/	(mV/	(mV vs (SCE)	(μA cm <sup>-2</sup> )	(mmpy)						
	decade)	decade)									
20 °C											
Uninhibited	-96.60	70.98	-209.31	73.56	0.84	-					
With DCHA	-103.76	83.72	-222.56	44.42	0.5390	39.61					
With MDEA	-101.38	75.00	-237.73	48.16	0.5573	34.53					
35 ℃											
Uninhibited	-119.95	98.45	-226.08	171.63	1.116	-					
With DCHA	-162.96	138.84	-228.00	113.22	1.29	34.03					
With MDEA	-109.23	84.08	-260.27	148.86	1.400	15.30					
45 °C											
Uninhibited	-114.17	81.60	-265.52	97.72	1.96	-					
With DCHA	-103.87	115.75	-224.12	84.06	1.686	13.98					
With MDEA	-106.45	105.43	-256.73	91.60	1.84	6.26					

DCHA = dicyclohexylamine, MDEA = n-methyldiethanolamine, VCI = volatile corrosion inhibitor

The results in Table 2 indicate that at 20 °C, the presence of inhibitors increased both  $|\beta_c|$  and  $|\beta_a|$ , implying that the inhibitors influenced both cathodic and anodic processes. With dicyclohexylamine being more effective, the corrosion potential,  $E_{\rm corr}$ , shifted anodically towards more positive potential. In inhibited specimens, the corrosion current density decreased and so is the corrosion rate. The dicyclohexylamine has higher corrosion inhibition efficiency than n-methyldiethanolamine.

## The effect of temperature on inhibited and uninhibited specimens of API X80 carbon steel specimens at 35 $^{\circ}C$

The polarisation curves results obtained when the corrosion tests were carried at elevated temperature of 35 °C have almost similar trend with those obtained at 20 °C as illustrated in Figure 6. The potentials in all

three curves are more negative than the potentials obtained at 20 °C indicating accelerated corrosion process with increasing temperature. This is also reflected in the decreased corrosion inhibition efficiency which was the direct effect of the significant increasing of corrosion current density. Dicyclohexylamine exhibited corrosion inhibition efficiency of 34.03 % while nmethyldiethanolamine's efficiency reduced to 15.30 % which is almost half of the efficiency obtained at 20 °C. This is an indication that *n*-methyldiethanolamine is less effective corrosion inhibitor at elevated temperature, whereas dicyclohexylamine efficiency was close to the efficiency obtained at 20 °C. This implies that the strength of the corrosion protective film of dicyclohexylamine at 35 °C was not affected with the increase in temperature.

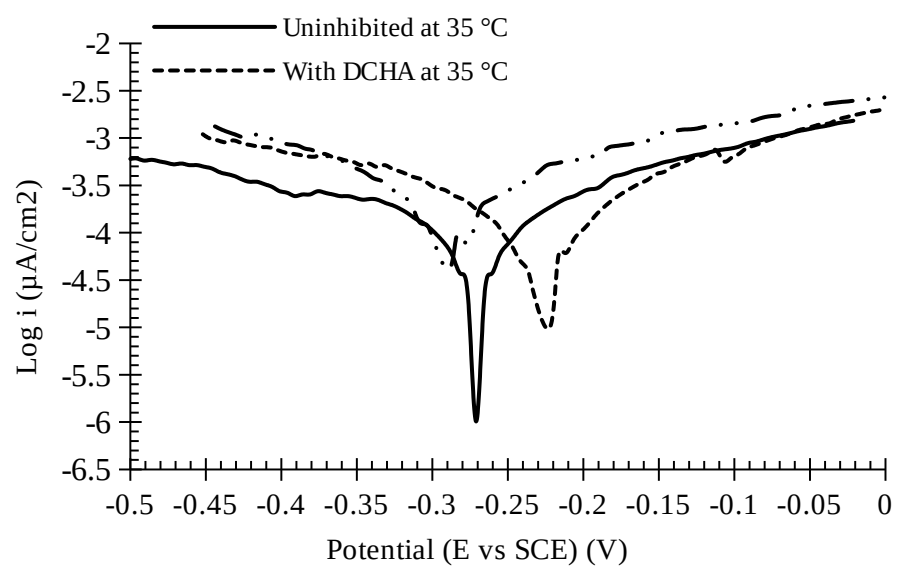


**Figure 6**: Tafel polarization curves for inhibited and uninhibited API X80 carbon steel specimens, recorded at  $35^{\circ}$ C and specimens exposed in CO<sub>2</sub> saturated electrolyte containing 200 ppm acetic acid and 1% NaCl. DCHA = dicyclohexylamine, MDEA = n-methyldiethanolamine

The results in Table 2 show that the presence of inhibitors raised  $\beta_a$  and decreased  $|\beta_c|$  values. With n-methyldiethanolamine on the surface of the working electrode, the corrosion potential,  $E_{\text{corr}}$ , shifted to the cathodic side while with dicyclohexylamine the  $E_{\text{corr}}$ , shifted anodically.

## The effect of temperature on the corrosion of inhibited and uninhibited API X80 carbon steel specimens at 45 °C

Tafel polarization curves obtained at 45 °C for inhibited and uninhibited the carbon steel API X80 specimens exposed in the same electrolyte are illustrated in Figure 7. The presence of dicyclohexylamine on the surface caused the open circuit potential to shift anodically, whereas *n*-methyldiethanolamine caused the open circuit potential to shift

cathodically relative to polarisation curve of uninhibited specimen. At 45 °C the corrosion inhibition efficiencies for both inhibitors were significantly small. Dicyclohexylamine which exhibited a significant corrosion inhibition efficiency at 20 °C and 35 °C, exhibited corrosion inhibition efficiency of 13.98 % at 45 °C. On the other hand, nmethyldiethanolamine exhibited a corrosion inhibition efficiency of 6.26% which means higher temperatures, the inhibitor protective film on the surface of the corrosion specimen could not provide inhibition. At elevated temperatures, the adsorption of volatile corrosion inhibitors onto the metal surface can be weakened, further reducing their protective action (Focke et al. 2013).

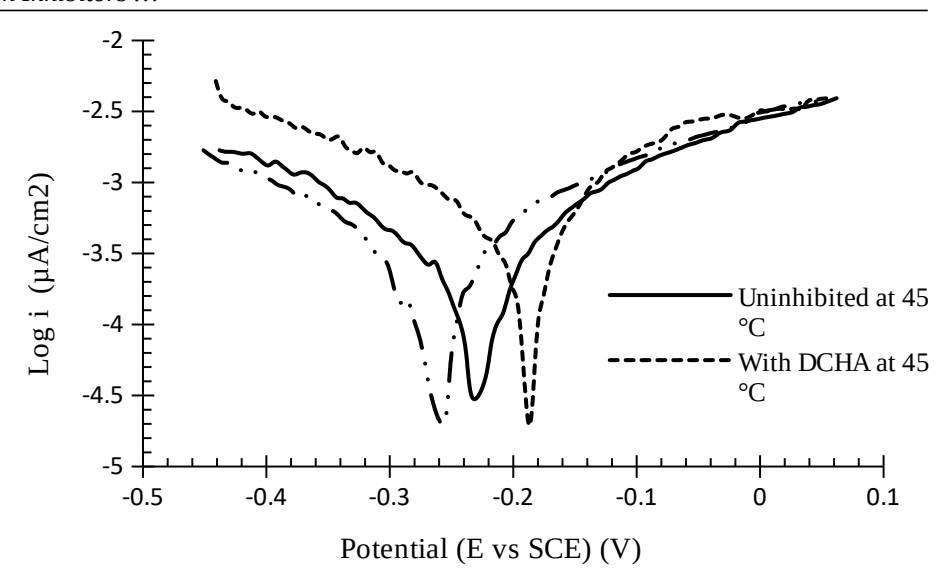


**Figure 7**: Tafel polarization curves for API X80 carbon steel specimens without and with volatile corrosion inhibitors on the surface, recorded at  $45^{\circ}$ C and specimens exposed in  $CO_2$  saturated electrolyte containing 200 ppm acetic acid and 1% NaCl. MDEA = n-methyldiethanolamine, DCHA = dicyclohexylamine

#### Conclusion

The results obtained from corrosion efficiency inhibition study of dicyclohexylamine and methyldiethanolamine on the selected carbon steel in aqueous CO<sub>2</sub>-saturated solutions containing 200 ppm acetic acid and 1% NaCl, have provided significant insights into their performance under varying temperature The findings revealed that conditions. dicyclohexylamine behaved as an anodic while *n*-methyldiethanolamine exhibited cathodic inhibition behaviour. This might be attributed by their difference in chemical structures which also affect their adsorption and hence the strength of the protective film on the metal surface. Dicyclohexylamine consistently demonstrated superior performance across all tested conditions over nmethyldiethanolamine. However, with increasing temperature the corrosion inhibition efficiencies of both inhibitors were dramatically reduced. The trend of corrosion inhibition efficiency decreased with increasing temperature such that the corrosion inhibition efficiencies of 39.61%, 34.03% and 13.98% upon dicyclohexylamine application and 34.53%, 15.30% and 6.26% with *n*-methyldiethanolamine were achieved at 20 °C, 35 °C and 45 °C respectively. This indicates there still a need for thermally stable volatile corrosion inhibitors capable of maintaining high inhibition efficiency under elevated temperature conditions in gas pipelines.

### Acknowledgement

The authors extend their sincere gratitude to the University of Dar es Salaam for granting Frida W. Andalu study leave and permission to travel to the University of Aberdeen to carry out research work. The authors are also grateful for the financial support provided by the Commonwealth Split-site Scholarships, which funded the experimental component of this research conducted at the University of Aberdeen in the United Kingdom. Special thanks are due to the School of Engineering at the University of Aberdeen for their technical valuable support encouragement during the data collection process.

### **Author Contributions**

W Frida Andalu: Fund acquisition, Methodology, Data analysis, writing original draft, Reviewing and Editing. Abraham K Temu: Conceptualization, Investigation, Data analysis, Writing, Reviewing and Editing, Supervision. Alfred R Akisanya: Conceptualization, Investigation, Data analysis, Writing, Reviewing and Editing, Supervision. Joseph YN Philip: Conceptualization, Investigation, Data analysis, Writing, Reviewing and Editing, Supervision.

### **Declaration of Competing Interest**

The authors declare that they have no known competing financial interests or personal relationships that could have appeared to influence the work reported in this paper.

### References

- Abbas A, Adesina AY and Suleiman RK 2023
  Influence of organic acids and related organic compounds on corrosion behaviour of stainless steel—A critical review. *Metals* 13: 1–25. https://doi.org/10.3390/met13081479
- Afsa 2011 Corrosion resistance of aluminium and protective measures where appropriate. *Aluminium Federation of South Africa*, South Africa. Corrosion-Pocket-Guide-February2011.qxd
- Alef K and Barifcani A 2020 Effect of N-methyl-diethanolamine and film forming corrosion inhibitor on gas hydrate, and empirical modelling for degradation. *J. Pet. Sci. Eng.* 184: 1–9. doi: https://doi.org/10.1016/j.petrol.2019.1065 22.
- Al-Janabi YT 2020 An overview of corrosion in oil and gas industry: upstream, midstream, and downstream sectors. In *Corrosion inhibitors in the oil and gas industry*, 1–38. Wiley-VCH Verlag GmbH & Co. KGaA. DOI: 10.1002/9783527822140.ch1
- Al-Moubaraki AH and Obot IB 2021 Top of the line corrosion: causes, mechanisms, and mitigation using corrosion inhibitors. *Arab. J. Chem.* 14: 1–27.

- https://doi.org/10.1016/j.arabjc.2021.1031
- Al-Moubaraki AH and Obot IB 2025 Mitigating top-of-the-line corrosion (TLC) using corrosion inhibitors: types and application methods. *Chem. Eng. Key* August 02. doi:
- 10.1016/j.arabjc.2021.103116
- Amani M and Hjeij D 2015 A comprehensive review of corrosion and its inhibition in the oil and gas industry. *Soc. Pet. Eng.* Mishref, Kuwait 1–14. https://doi.org/10.2118/175337-MS
- Askaria M, Aliofkhazraei M and Afroukhteh S 2019 A comprehensive review on internal corrosion and cracking of oil and gas pipeline. *J. Nat. Gas Sci. Eng.* 71: 1–25. A comprehensive review on internal corrosion and cracking of oil and gas pipelines | Scinito
- Bai Y and Bai Q 2014 *Subsea pipeline integrity management*. Gulf Professional Publishing, Waltham, USA. Subsea pipeline integrity and risk management: Bai, Yong, Bai, Qiang: Amazon.in: Books
- Belarbi Z, Farelas F, Singer M and Nesic S 2016 Role of amine in the mitigation of  $CO_2$  top of the line corrosion. *Corros.* 2016 Conf. Expo 1300–1310. https://doi.org/10.5006/2121
- Cano E, Bastidas DM, Simancas J and Bastidas J M 2005 Dicyclohexylamine nitrite as volatile corrosion inhibitor for steel in polluted environments. *Corros. Sci.* 61(5): 473–479. https://doi.org/10.5006/1.3280647
- Eslami M and Singer M 2023 Influence of experimental injection method on the inhibition efficiency of volatile corrosion inhibitors on top of line corrosion. *AMPP Annu. Conf. Expo*, Denver, Colorado. https://onepetro.org/amppcorr/proceeding s-abstract/AMPP23/AMPP23/AMPP-2023-19452/527148
- Gunasekarana P, Veawab A and Aroonwilas A 2016 Corrosivity of amine-based absorbents for  $CO_2$  capture. *GHGT-13 Conf.* 14–18. ivecommons.org/licenses/by-nc-nd/4.0/).
- © 2017 The Authors. Published by Elsevier Ltd.

- Wan HJ, Huang HJ, Zhang M and Li ZG 2005 A modified method for evaluation of materials containing volatile corrosion inhibitor. *J. Cent. South Univ. Technol.* 12(4): 406–410. DOI: 10.1007/s11771-005-0172-0
- Ituen EB and Asuquo JE 2019 Inhibition of X80 steel corrosion in oilfield acidizing environment using 3-(2-chloro-5,6-dihydrobenzo[b][1] benzazepin-11-yl)-N, N dimethylpropan-1-amine and its blends. *J. King Saud Univ. Sci.* 31: 127–135. http://dx.doi.org/10.1016/j.jksus.2017.06.009
- Jevremovic I, Debelikovic A and Singer M 2012 A mixture of dicyclohexylamine and oleylamine as a corrosion inhibitor for mild steel in NaCl solution saturated with CO<sub>2</sub> under both continual immersion and top of the line corrosion. *J. Serb. Chem. Soc.* 77(8): 1047–1061. https://doi.org/10.2298/JSC120222058J
- Khamis E, Oun S R and Lyon SB 2001 Use of dicyclohexylamine nitrite in inhibition of coupled zinc and steel. *Br. Corros. J.* 36(3): 197–200. DOI: 10.1179/000705901322914070
- Kolawole FO, Kolawole SK, Agunsoye JO, Adebisi JA, Bello SA and Hassan S B 2018 Mitigation of corrosion problems in API 5L steel pipeline a review. *J. Mater. Environ. Sci.* 9(8): 2397–2410. http://www.jmaterenvironsci.com!
- Konovalova V 2020 The effect of temperature on the corrosion rate of iron-carbon alloys. *Mater. Today* 38(4): 1326-1329.
  - https://doi.org/10.1016/j.matpr.2020.08.09 4Get rights and content
- Mungwari CP, Obadele BA and King'ondu CK 2024 Phytochemicals as green and sustainable corrosion inhibitors for mild steel and aluminium: review. *Results Surf. Interfaces* 18(1): 1–19. DOI: 10.1016/j.rsurfi.2024.100374
- Nan Z 2021 Corrosion failure behavior analysis and countermeasures of gas transmission pipeline. *IOP Conf. Ser.: Earth Environ. Sci.*, 651(2021) Xinjiang, China. doi:10.1088/1755-1315/651/3/032025

- Niu L and Cheng YF 2008 Development of innovative coating technology for pipeline operation crossing the permafrost terrain. *Constr. Build. Mater.* 22(4): 417–422. doi: https://doi.org/10.1016/j.conbuildmat.200 7.06.001
- Palanisamy G 2019 Corrosion inhibitors. In *Surface science*, 1–24. IntechOpen, Nagaland University, India. DOI: 10.5772/intechopen.80542
- Popoola LT, Grema A S, Latinwo GK, Gutti B and Balogun AS 2013 Corrosion problems during oil and gas production and its mitigation. *Int. J. Ind. Chem 4(1)*:: 1–15. DOI: 10.1186/2228-5547-4-35
- Liu Q, Yang S, Zhao M, Zhu L and Li J 2017 Pitting corrosion of steel induced by  ${\rm Al_2O_3}$  inclusions. *Metals* 347(7): 1–12. https://doi.org/10.3390/met7090347
- Ramlan DG, Juli NB, Pojtanabuntoeng T and Yaakob N 2024 Benzylamine as volatile corrosion inhibitor for top-of-the-line corrosion in water-hydrocarbon cocondensation environment. *J. Pipeline Sci. Eng* 5(3): 1–33. https://doi.org/10.1016/j.jpse.2024.10025
- Rostron P and Kasshanna S 2015 Novel synthesis of vegetable oil derived corrosion inhibitors. *Int. J. Corros.* 2015: Article ID 851698 1–7. http://dx.doi.org/10.1155/2015/851698
- Shahzad K, Sliem MH, Shakoor RA, Radwan BA, Kahraman R, Umer MA, Manzoor U and Abdullah AM 2020 Electrochemical and thermodynamic study on the corrosion performance of API X120 steel in 3.5% NaCl solution. *Sci. Rep.* 10: Article 61139. doi: 10.1038/s41598-020-61139-3
- Tong Y, Ye J, Wang Q, Zhang H, Yu H and Seibou AO 2023 Ethanolamines corrosion inhibition effect on steel rebar in simulated realkalized concrete environments. *J. Asian Archit. Build. Eng.* 22(2): 415–424. https://doi.org/10.1080/13467581.2024.23 57197
- Valente MAG Jr, Gonçalves LM, Passaretti Filho J, Cardoso AA, Rodrigues JA, Fugivara CS and Benedetti AV 2020

- Corrosion protection of steel by volatile corrosion inhibitors: vapor analysis by gas-diffusion microextraction and mass loss and electrochemical impedance in NaCl deliquescence tests. *J. Braz. Chem. Soc.* 31(10): 2039–2048. DOI: 10.21577/0103-5053.20200104
- Wang D 2022 Heat loss along the pipeline and its control measures. *SN Appl. Sci.* 5(2): 1–14. DOI: 10.1007/s42452-022-05226-2
- Wint D and Williamson TD 2014 Multifaceted approaches for controlling top-of-the-line corrosion in pipelines. *SPE Int. Oilfield Corros. Conf. Exhib.*, Aberdeen. DOI: 10.2118/169630-MS. https://www.researchgate.net/publication/267461236
- Xiao K, Li Z, Song J, Bai Z, Wei X, Wu J and Dong C 2020 Effect of concentrations of Fe<sup>2+</sup> and Fe<sup>3+</sup> on the corrosion behavior of carbon steel in Cl<sup>-</sup> and SO<sub>4</sub> aqueous

- environments. *Met. Mater. Int* 27(8): 1–11. 10.1007/s12540-019-00590-y
- Xue HB and Cheng YF 2011 Characterization of inclusions of X80 pipeline steel and its correlation with hydrogen-induced cracking. *Corros. Sci.* 53(4): 1201–1208. 10.1016/j.corsci.2010.12.011
- Yonova D and Fachikov L 2007 Influence of aluminium ions on corrosion of galvanized steel used in heating systems. *J. Univ. Chem. Technol. Metall.* 42(1): 73–76.
  - https://journal.uctm.edu/node/j2007-1/12-Fachikov-73-76.pdf
- Zankana MM, Muhammed SH, Barzinjy AA, Abdulrahman AF and Mousa MS 2023 A comprehensive comparative study of some corrosion inhibitors using different techniques. *Hybrid Adv.* 4: 1–9.
  - DOI: 10.1016/j.hybadv.2023.100099.